The phase diagram and magnetic properties of $La_{1-x}Ca_xMnO_3$ compounds for $0 \leq x \leq 0.23$

2004 J. Phys.: Condens. Matter 16 6527

(http://iopscience.iop.org/0953-8984/16/36/018)

INSTITUTE OF PHYSICS PUBLISHING JOURNAL OF PHYSICS: CONDENSED MATTER

J. Phys.: Condens. Matter **16** (2004) 6527–6540 PII: S0953-8984(04)78210-7

The phase diagram and magnetic properties of $La_{1-x}Ca_xMnO_3$ compounds for $0 \leqslant x \leqslant 0.23$

M Pissas and G Papavassiliou

Institute of Materials Science, NCSR, Demokritos, 153 10 Aghia Paraskevi, Athens, Greece

Received 22 March 2004
Published 27 August 2004
Online at stacks.iop.org/JPhysCM/16/6527
doi:10.1088/0953-8984/16/36/018

Abstract

In this paper a detailed study of the $La_{1-x}Ca_xMnO_3$ ($0 \leqslant x \leqslant 0.23$) phase diagram using powder x-ray diffraction and magnetization measurements is presented. The lack of well characterized samples has resulted in confusion as regards the underlying physics of this complicated system. As the present study reveals, two distinct families of samples exist. The first family consists of samples prepared in an air atmosphere (designated as AP; $P(O_2) = 0.2$ atm). These are ferromagnetic with their Curie temperatures increasing with x. The second family of samples consists of samples prepared in air and then post-annealed under a reducing nearly zero oxygen partial pressure (designated R). These samples show a canted antiferromagnetic structure for $0 \leqslant x \leqslant 0.1$ below T_N, while for $0.125 \leqslant x < 0.23$ an unconventional ferromagnetic insulated phase is present below T_c. Most probably, the difference between the two families of samples, R and AP, lies in their cation stoichiometries, the AP samples being stoichiometric and the AP samples being non-stoichiometric. The most important difference between AP and R samples is the anisotropy in the exchange interactions of the R samples. This leads us to suggest the possibility that a new orbital ordered phase is responsible for the ferromagnetic insulating regime in the $La_{1-x}Ca_xMnO_3$ compounds.

(Some figures in this article are in colour only in the electronic version)

1. Introduction

The manganite perovskites $RE_{1-x}AR_xMnO_3$ (RE = La and rare earths, AR = Ca, Sr, Ba) display interesting and puzzling structural, magnetic and transport properties. The reason for this is the close interplay between charge, spin and lattice degrees of freedom. One of the most popular systems studied in detail, as regards the transport, structural and magnetic properties [1–8], is the Ca-based $La_{1-x}Ca_xMnO_3$ ($0 \leqslant x \leqslant 1$) compounds. In stoichiometric $LaMnO_3$ at T_{RO}, a structural rhombohedral to orthorhombic transition occurs. In the orthorhombic phase the MnO_6 octahedra exhibit a specific tilting system governed by

the particular value of the tolerance factor. Mn^{3+} ions in an undistorted octahedral oxygen coordination have an electronic structure $d^4 = t_{2g}^3 e_g^1$ (one electron in a doubly degenerate e_g orbital).

At T_{JT}, $LaMnO_3$ is transformed from the basic orthorhombic (O) to another orthorhombic structure (O′). In the O phase the three octahedral MnO bond lengths are almost equal. The transition at T_{JT} originates from a cooperative Jahn–Teller (JT) structural transition [9, 10] resulting in anisotropic Mn–O bond lengths, with the long bond ordered in a two-sublattice fashion [11] in the *ac* plane. This particular ordering of the long bonds in the basal *ac* plane (*Pnma* notation) has been connected with the orbital ordering of the d_{x^2} and d_{z^2} orbitals. Finally, at T_N the compound is ordered antiferromagnetically, exhibiting the so-called A antiferromagnetic structure (**m** $\parallel$ *a*-axis) where ferromagnetic layers are coupled antiferromagnetically along the *b*-axis. This ordering system is due to orbital ordering. The antiferromagnetic interactions along the *b*-axis are related to the three t_{2g} electrons. The strong overlap between the half-filled orbitals d_{x^2} at site 1 and the empty one $d_{x^2-y^2}$ at site 2 gives the ferromagnetic exchange [10] (in the *ac* plane, in accordance with the Goodenough–Kanamori–Anderson rules).

The replacement of La by Ca, i.e. doping the compound with hole-like charge carriers, induces drastic changes of the structural and magnetic/transport properties. At the doping level $0.0 < x \leqslant 0.1$ the long range magnetically ordered state for $T < T_c$ is a canted antiferromagnetic structure (CAF). This structure is closely connected to the A antiferromagnetic structure of the $LaMnO_3$ compound where the collinear magnetic moments in the *ac* plane are canted in such a way as to produce a net ferromagnetic component along the *b*-axis [12]. The anisotropy of the Mn–O bond lengths in the O′ phase is still present with a tendency for it to reduce as x increases. Based on the assumption that this ordering of the long bonds is connected with the orbital ordering, the orbital ordering is preserved in the CAF regime.

With further doping $0.125 < x < 0.23$, the CAF phase is transformed to a ferromagnetic insulating phase, contradicting the conventional double-exchange and superexchange models. Up to 80 K this phase follows the O′ structure [13] with moderately anisotropic Mn–O bond lengths. As the doping concentration x increases, the static JT distortion weakens progressively and the system becomes metallic and ferromagnetic for $x > 0.23$. It is believed that in the absence of a cooperative effect in this regime, local JT distortions persist [14–16] on short scales of time and length. These short range correlations, together with the electron correlations, may create the effective carrier mass necessary for large magnetoresistance.

The ferromagnetic insulating phase is one of the most puzzling regimes in the physics of manganite perovskites. Several models have been proposed for interpreting it, especially for the $La_{1-x}Sr_xMnO_3$ compound, using new orbital and charge ordering [17, 18] states. Although a lot of experimental studies have been devoted to the ferromagnetic insulating regime of the $La_{1-x}Ca_xMnO_3$ compound, in most of them significantly non-stoichiometric samples have been used. As the crystal chemistry and physical properties of the low Ca content samples depend on the partial pressure of the oxygen during the sample preparation, this leads (as has been pointed out by Dabrowski *et al* [19]) to contradictory results being published by different groups. The non-stoichiometric samples, although showing ferromagnetic insulating behaviour for $x < 0.2$, most probably contain cation vacancies where the orbital order of the ferromagnetic insulating regime is probably a short range or liquid state. In addition, the concentration gradients in the published data on single crystals (when they are free of vacancies) make direct comparison of the results between different compositions and research groups difficult. As the results of the present study reveal, there are basically two families of samples. The first family of samples, AP, displays ferromagnetic behaviour with Curie temperatures

which diminish as x goes to zero. The second family of samples, R, have a complicated phase diagram. A first attempt at understanding how the preparation conditions influence the phase diagram of $La_{1-x}Ca_xMnO_3$ ($0 \leqslant x \leqslant 0.2$) has been performed by Dabrowski *et al* and Huang *et al*, in [19–21]. In these studies the role of the oxygen partial pressure has been recognized as the key parameter influencing the Mn^{4+} concentration in addition to the nominal calcium content. Taking into account these observations, one must be cautious in adopting theoretical models before the basic solid state chemistry is understood and the complete characterization of the $La_{1-x}Ca_xMnO_3$ compound is achieved.

In the present paper we carry out a detailed study of the bulk magnetic properties of $La_{1-x}Ca_xMnO_3$ ($0 \leqslant x \leqslant 0.23$) with two sets of samples, in an effort to elucidate the complications that originate from the non-stoichiometry of the samples.

2. Experimental details

$La_{1-x}Ca_xMnO_3$ samples were prepared by thoroughly mixing stoichiometric amounts of preheated La_2O_3, $CaCO_3$ and MnO_2, following a solid state reaction method, in air at 1400 °C. We call these samples 'air prepared' (AP). A part of each AP sample was subsequently post-annealed at 1000–1150 °C (depending on x) [19] in a high purity He flow. These samples are called reduced samples (R). X-ray powder diffraction (XRD) data were collected with a D500 SIEMENS diffractometer, using Cu Kα radiation. The Rietveld refinement of the XRD data was performed by using the FULLPROF program [22]. DC magnetization measurements were performed in a superconducting quantum interference device (SQUID) magnetometer (Quantum Design MPMS2). For ac susceptibility measurements a home-made susceptometer was employed. The dc, the drive and pickup coils are inside the cryogenic fluid to achieve measurements in a constant temperature background. All the ac susceptibility measurements presented in this paper were performed under an ac magnetic field 2.25 Oe and at frequency 1111 Hz, except those of figure 7 where $f = 111.1$ Hz was used.

3. X-ray diffraction data

Figure 1 shows parts of the XRD patterns of the AP and R samples. On the basis of the Rietveld method, both set of samples can be structurally described using the *Pnma* space group. In addition, the R samples display cooperative Jahn–Teller structure, which is characterized by the splitting of (101) and (020) diffraction peaks. As the Rietveld refinement revealed, in each MnO_6 octahedron there are three different bonds, with the medium length Mn–O_1 bond (m) directed along the b-axis and the long (l) and short (s) Mn–O_2 bonds alternating along the a- and c-axes (*Pnma* notation).

XRD data for all AP samples show single-phase samples. No cooperative Jahn–Teller distortion is present for the AP samples, as revealed by the unit cell constants and the Mn–O bond lengths, even for samples with $x < 0.1$. *Most probably, all these AP samples are cation deficient samples*. One may argue that the oxygen content for this family of samples may be larger than for the stoichiometric samples. However, the $LaMnO_3$ perovskite-type structure is a close-packed LaO_3 lattice with the Mn ions in the octahedral sites completely surrounded by oxygen ions. The possible sites for interstitial ions (tetrahedral and octahedral) are surrounded by negatively charged ions (oxygens) as well as by positively charged ions (lanthanum). It is very hard to incorporate charged particles into these sites. Consequently, a cation vacancy structure [20] can explain the variation of the crystal chemistry and the physical properties of the $La_{1-x}Ca_xMnO_3$ system for $0 \leqslant x \leqslant 0.23$. Most importantly, refining the atomic

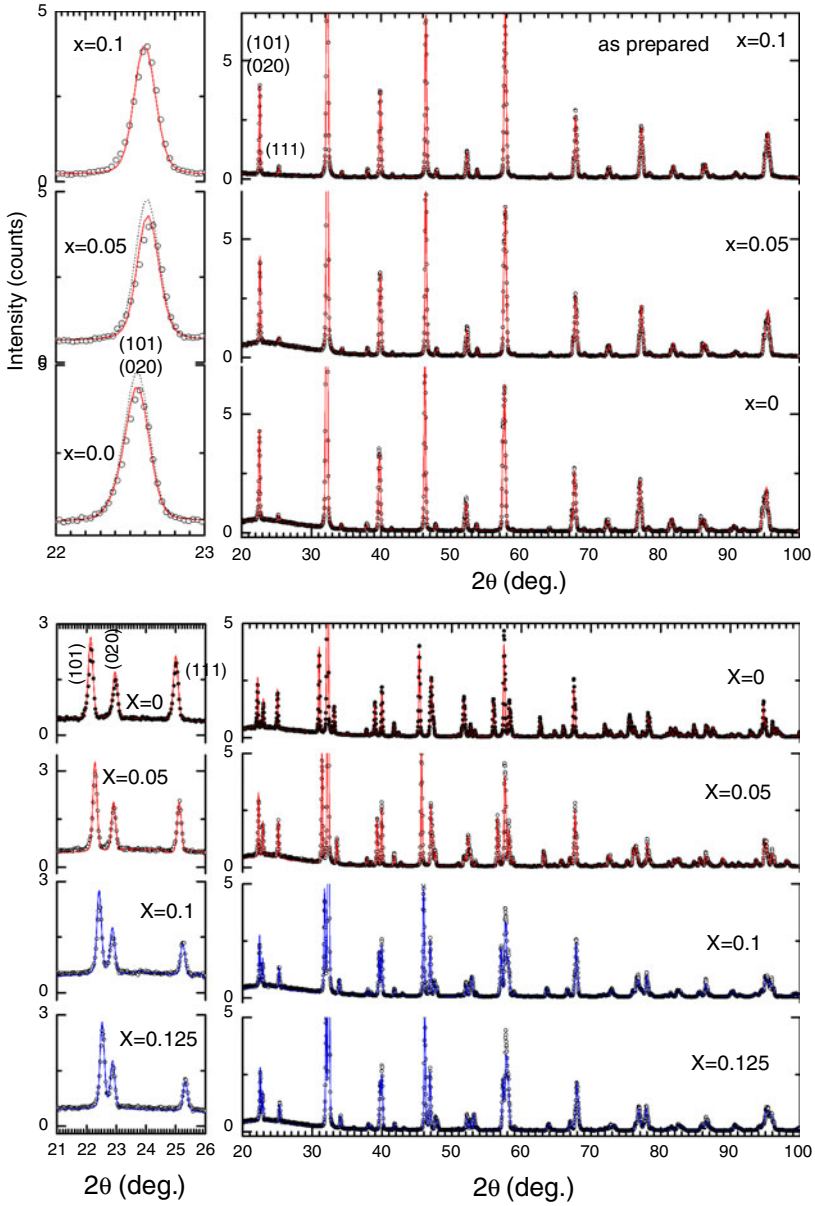

Figure 1. X-ray diffraction patterns for $La_{1-x}Ca_xMnO_3$ samples prepared in air atmosphere at 1400° (upper panel) and $La_{1-x}Ca_xMnO_3$ samples post-annealed at 1000 °C in high purity He (lower panel). To the left of the main panel is a magnified view of the patterns near the (101), (020) reflections.

positional and isotropic thermal parameters and retaining the occupancy factors according to the nominal composition did not yield a completely satisfactory refinement because some peaks (e.g. (101), (020)) did not have adequate intensity. On including as additional free parameters the occupation factors for La and Mn, a clear improvement of the fit was achieved, with the fitted peaks giving the right intensities. The results of the refinement show clearly

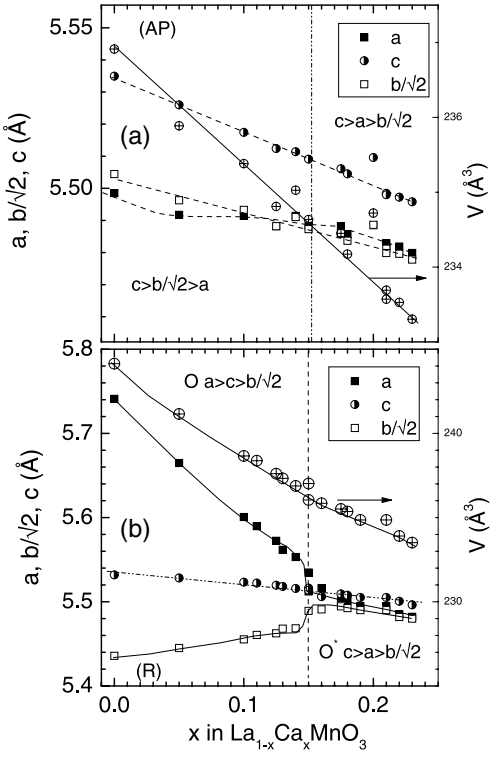

Figure 2. (a) The concentration dependences of the unit cell parameters and volumes for AP (a) and R (b) $La_{1-x}Ca_xMnO_3$ samples.

that nearly equal amounts of La and Mn vacancies are present in the AP samples. The La and Mn deficiency decreases as x increases.

Figure 2 shows the concentration variation of the unit cell parameters for AP and R samples. While for the AP samples the cell constants decrease monotonically as x increases, the corresponding variation for the R samples shows a clear change in the slope at around $x \approx 0.15$. For higher x there is no very substantial difference between the variations of the cell constants of the AP and R samples. It is interesting to note that the unit cell volume changes monotonically with x as expected from the smaller ionic radii of the Ca^{2+} and Mn^{4+}. However, the slope differs by a factor of two between the two families of samples; e.g. $(\mathrm{d}(V/V_0)\,\mathrm{d}x = -0.1455$ for AP samples and $\mathrm{d}(V/V_0)\,\mathrm{d}x = -0.27$ for the R samples (V_0 is the unit cell volume at $x = 0$ for the AP and R samples)). The difference in unit cell reduction slope is most probably related to the cooperative Jahn–Teller distortion, which is present only for the R samples. The abrupt changes of the unit cell parameters for $x < 15$ are the result of the intersections of the Jahn–Teller transition curve (for $x < 0.15$, $T_{\mathrm{JT}}(x) > 300$ K). Both families of samples exhibit a $GdFeO_3$ distortion of the perovskite structure. Orthorhombic perovskites have been separated into type O* ($b/c > \sqrt{2}$, *Pnma* notation), wherein the predominant distortion is octahedral tilting as in $GdFeO_3$, and type O′ ($b/c < \sqrt{2}$), wherein the predominant distortion is driven by the cooperative Jahn–Teller effect. The R samples at $T = 300$ K up to $x = 0.15$ are described by the O′ structure. We must note that the difficulty in preparing homogeneous samples in the $x = 0.15$ region is related to the fact that the cooperative JT distortion, around this particular concentration, occurs near $T = 300$ K. It should be noted that change of the

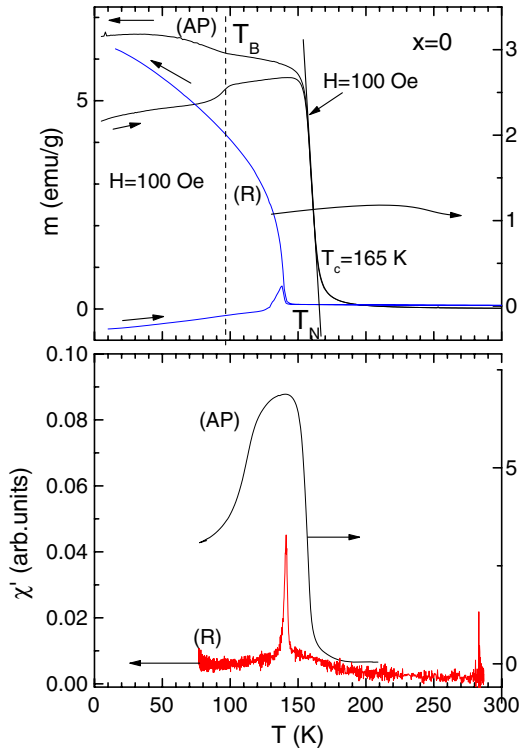

Figure 3. The temperature dependence of the dc magnetic moment (upper panel) and initial ac susceptibility (lower panel) for the AP and R $LaMnO_3$ samples. The dc magnetic moment was measured in ZFC and FC modes (see the main text).

magnetic state of $La_{1-x}Ca_xMnO_3$ owing to the oxygen content has also been observed for $x = 0.3$ and 0.5 by Trukhanov *et al* [23]. In this study the modifications of the magnetic properties are related to the oxygen vacancies, producing a reduction of the ferromagnetic transition temperature and a cluster spin glass state in place of the ferromagnetic state.

4. Magnetic measurements

Proceeding further, we carried out both dc magnetic moment and ac susceptibility measurements in order to estimate the magnetic phase diagrams of the two families of samples. Figure 3 shows the temperature dependence of the magnetic moment for both AP and R $LaMnO_3$ samples. The AP sample shows a paramagnetic to ferromagnetic transition at $T_c = 165$ K. The temperature variation of the magnetic moment shows strong irreversible behaviour depending on the measuring mode. In the zero-field cooling mode (ZFC) the moment initially increases slightly up to 80 K. In a relatively narrow temperature interval a step-like increase of the magnetic moment is observed. We characterize this feature by its onset temperature, during cooling, denoted by T_B. Subsequently the moment increases up to 150 K and then sharply decreases at the Curie temperature. The width of the transition at T_c is relatively sharp in comparison with ferromagnetic–paramagnetic transitions observed at higher concentrations. The sharpness of the transition may imply a first-order magnetic transition. However, the absence of measurable hysteresis in this regime does not favour a clear first-order transition. On cooling under a magnetic field, the magnetic moment below 150 K

shows pronounced irreversible behaviour. This thermal irreversibility of the magnetization is observed below T_{irr}; this is a common feature of all kinds of magnetic systems showing magnetic hysteresis behaviour. At T_B the FC branch displays a slope change, with the result that the moment for $T < T_B$ rises more rapidly than that for above T_B. This general shape of the $m(T)$ curve appears for all AP samples for $0 \leqslant x \leqslant 0.2$ (see below).

The lower panel of figure 3 shows the real part of the ac susceptibility for both the AP and R samples. Let us first examine the data for AP sample. Below the Curie temperature, $\chi'(T)$ increases down to the temperature where the ZFC and FC branches of the dc moment display hysteretic behaviour. Below this temperature, $\chi'(T)$ decreases rapidly and finally becomes nearly horizontal for $T < T_B$. The corresponding imaginary part (not shown) shows two peaks: one at T_c and the other at T_B. It is interesting to note that the ac susceptibility measurements do not show irreversible behaviour during heating and cooling. The R sample shows radically different behaviours. Both the ac susceptibility and the dc magnetic moment show a lower transition temperature $T_c = 145$ K. The ZFC and FC branches of the $m(T)$ curve show strongly irreversible behaviour from T_c, with the ZFC branch far below the FC one. Isothermal magnetization measurements at $T = 5$ K (not shown) revealed behaviour typical of a canted antiferromagnet, which is in agreement with neutron diffraction measurements [6] (the neutron diffraction data mainly show an A-type antiferromagnetic structure because the ferromagnetic component is very small). The real part of the external susceptibility (uncorrected for demagnetizing effects) $\chi'(T)$ displays a very narrow peak at the transition temperature.

In the case of a canted antiferromagnet the ac susceptibility along the ferromagnetic axis (e.g. the b-axis in our case), is expected to diverge above and below T_N. On the other hand, the ac susceptibility along the other orthogonal axes displays the usual behaviour for an antiferromagnetic material. In our powder sample the response is governed by the divergent part which is larger than the antiferromagnetic one. For a canted antiferromagnet the susceptibility is expected to diverge over the interval $\Delta T = (T_N - T_0)/T_N$ where $\Delta T = (D/\sum_i |J_i|)^2$, T_0 is the temperature where the susceptibility begins to diverge and D is the anisotropy constant of crystal field-type DS_z^2 or Dzyaloshinskii–Moriya interactions [24]. The sharp fall in χ' below T_N can be ascribed to the onset of coercivity. As x increases (samples 0.05 and 0.1) the magnetic measurements for both AP and R samples are practically the same as those for the $LaMnO_3$ sample. It is interesting to note that the width of the susceptibility peak increases with x, a fact which may be related to a softening of $(\sum_i |J_i|)^2$ with x. In figure 4 the dc magnetic moment and ac susceptibility measurements are plotted for the $x = 0.1$ samples in order to emphasize the differences from the $x = 0.0$ sample results. The AP sample shows exactly the same behaviour as the corresponding $x = 0.0$ sample except for a slightly higher T_c. The R sample continues to show behaviour characteristic of a canted antiferromagnet.

The magnetic measurements on the AP sample with $x = 0.11$ show similar behaviour to those for all the previous AP samples. The χ' of the R $x = 0.11$ sample shows two features in place of the single peak observed for $x \leqslant 0.1$. On the high temperature side of the peak of χ', a clear shoulder appears, indicating that this sample displays two transitions. The transition located at the peak is most probably related to the CAF transition of the $x = 0.1$ sample, while the shoulder is most probably related to a ferromagnetic transition. Similar behaviour has been observed by Biotteau *et al* [6] using neutron data for a single crystal with $x = 0.1$. Figure 5 shows the dc magnetic moment and ac susceptibility measurements for both AP and R $x = 0.125$ samples. The situation for the R $x = 0.125$ sample is clearer. Here, a ferromagnetic transition at $T_c \approx 150$ K and a shoulder at 115 K (see the arrow in figure 5) are observed. We attribute the shoulder to an antiferromagnetic transition which occurs in this sample a little below T_c. The dc magnetic moment displays hysteretic behaviour below $T_{irr} \approx 140$ K, between

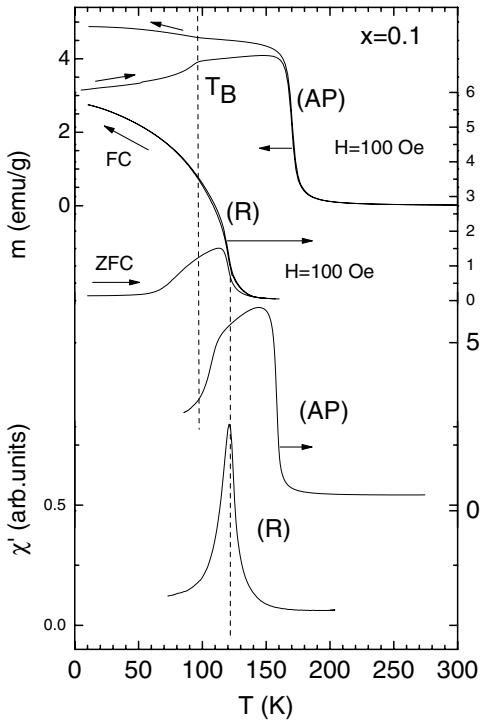

Figure 4. The temperature dependence of the dc magnetic moment and the initial ac susceptibility for the AP and R $La_{0.9}Ca_{0.1}MnO_3$ samples. The dc magnetic moment was measured in ZFC and FC modes (see the main text).

the ZFC and FC branches. The ZFC branch increases non-linearly with temperature and does not exhibit any other feature. At $T = 115$ K $\equiv T_N$ it displays a maximum. All the R samples for the range $0.011 < x < 0.15$ display the peak at T_c in the χ' accompanied by a shoulder. For $x > 0.15$ the shoulder is replaced by a broad shoulder. For $T < 80$ K, χ' becomes nearly horizontal. For $x > 0.15$ the dc magnetic measurements are not essentially different from those for the AP samples, except for the lower T_c of the R samples. The step-like increments of the magnetic moment in the ZFC branches are present for both families of samples. The ac susceptibility measurements for the R samples show an asymmetric peak at T_c and a small reduction in the temperature region where the step-like variation of the dc moment occurs. A representative example is shown in figure 6 for the $x = 0.19$ sample. For the R $x = 0.19$ sample the dc magnetic measurements show irreversibility at $T_{irr} \approx 180$ K and a step at T_B. The corresponding $\chi'(T)$ shows an asymmetric peak at T_{irr}, then decreases and finally forms a shoulder at T_B before becoming horizontal.

The ac susceptibility for the samples with $x > 0.14$ increases rapidly as T_c is approached from above, passing though a maximum at a temperature somewhat below T_c. This maximum originates from the Hopkinson effect [25] and not from critical effects. The Hopkinson effect is due to the rapid increase in anisotropy with decreasing temperature below T_c, particularly when its value begins to exceed the ac field [26]. The application of an external static biasing field results in a rapid suppression of both the amplitude and the temperature of this principal maximum. The measurements under a dc field revealed a smaller secondary peak, which decreases in amplitude and moves upward in temperature as the applied field increases. This feature is a direct manifestation of critical fluctuation in a system approaching a second-

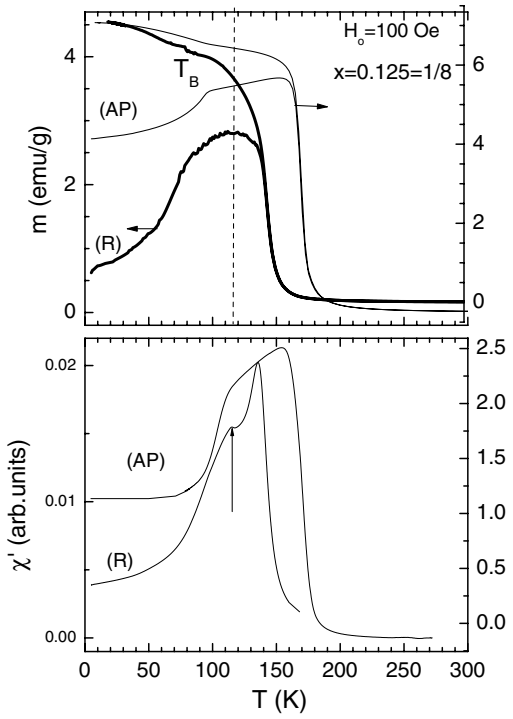

Figure 5. The temperature dependence of the dc magnetic moment (upper panel) and initial ac susceptibility (lower panel) for the AP and R $La_{0.875}Ca_{0.125}MnO_3$ samples, respectively.

order paramagnetic to ferromagnetic transition and it is uniquely revealed by susceptibility measurements. This behaviour is clearly shown in figure 7 for the $x = 0.19$ R sample. We would like to point out that a pronounced Hopkinson peak is absent for the AP sample and for both families of samples for $x > 0.2$.

Our magnetic measurements for the R $x = 0.19$ sample are in good agreement with the single-crystal data of Hong *et al* [27]. The anomaly at T_B was attributed to freezing of a cluster glassy phase which appears below T_c. According to their neutron diffraction data this glassy phase accounts for 0.4 μ_B per Mn ion and has to do with charge/orbital fluctuations. For $x > 0.2$ both families of samples show behaviour typical for a low anisotropy soft ferromagnetic material.

5. Phase diagram

On the basis of the magnetic measurements, the magnetic phase diagrams for both families of $La_{1-x}Ca_xMnO_3$ samples were determined and these are plotted in figure 8. The AP samples display a ferromagnetic transition at $T_c(x)$, which increases with x (see figure 8(a)). In this figure the onset points $T_B(x)$, where the step increment of the magnetic moment is observed, are also plotted. This transition temperature $T_B(x)$ is nearly independent of x. Although this transition persists for $x > 0.2$ the height of the magnetic moment 'jump' diminishes significantly. The physical origin of T_B is the subject of several recent publications but its complete elucidation has not yet been achieved. Figure 8(b) shows the phase diagram of the R samples which is radically different from that for the AP samples, especially for $x < 0.15$.

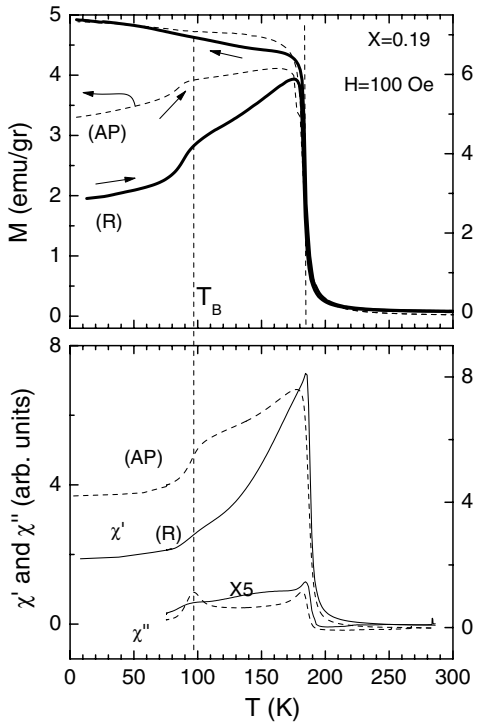

Figure 6. The temperature dependence of the dc magnetic moment (upper panel) and initial ac susceptibility (lower panel) for the AP and R $La_{0.81}Ca_{0.19}MnO_3$ samples, respectively.

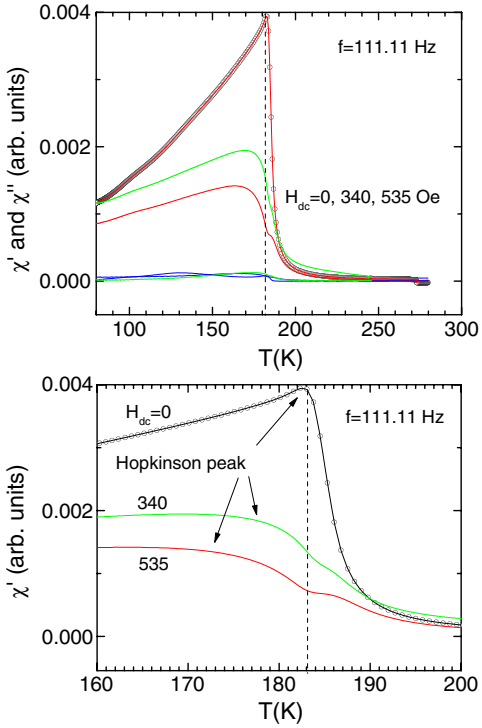

Figure 7. The temperature variation of the linear fundamental ac susceptibility for various dc fields for the $x = 0.19$ R sample. The lower panel shows the details of the measurements near T_c.

Our results for the R samples are in good agreement with those of [6, 28], where stoichiometric single crystals were studied. For $0 \leqslant x < 0.125$ the R samples undergo a transition from a paramagnetic to a canted antiferromagnetic state at T_N. The $x = 0$ sample is an A_x-type antiferromagnet with a small ferromagnetic component along the b-axis ($Pnma$ notation). As x increases the ferromagnetic component of the canted magnetic structure increases at the expense of the antiferromagnetic phase. For $x > 0.08$ it is clear that antiferromagnetic and ferromagnetic transitions occur at different temperatures ($T_N < T_c$). For $0.125 \leqslant x \leqslant 0.2$, according to the magnetic saturation measurements all the samples show ferromagnetic behaviour. However, the real character of the zero-field ground state is not clear. The dc magnetic and ac susceptibility measurements show a rather complex behaviour. Let us describe the possible physical origin of the special features observed in magnetic measurements for R samples. Figure 9 clearly shows this behaviour. We have plotted $\chi'(T)$ for all the R samples. The first transition appears as a peak and has to do with the ferromagnetic interactions of the canted structure for $0.125 < x \leqslant 0.15$. Subsequently, instead of the peak decreasing, as for the CAF structure, after a broad shoulder it remains temperature independent down to zero temperature. At the same time the dc magnetic moment presents a smaller difference between the ZFC and FC branches in comparison to the CAF structure. All these observations imply that we have a behaviour where the mechanism responsible for the CAF structure weakens progressively for $x > 0.125$. It seems that the shoulder related to T_N for $x < 0.125$ is transformed to a feature at T_B.

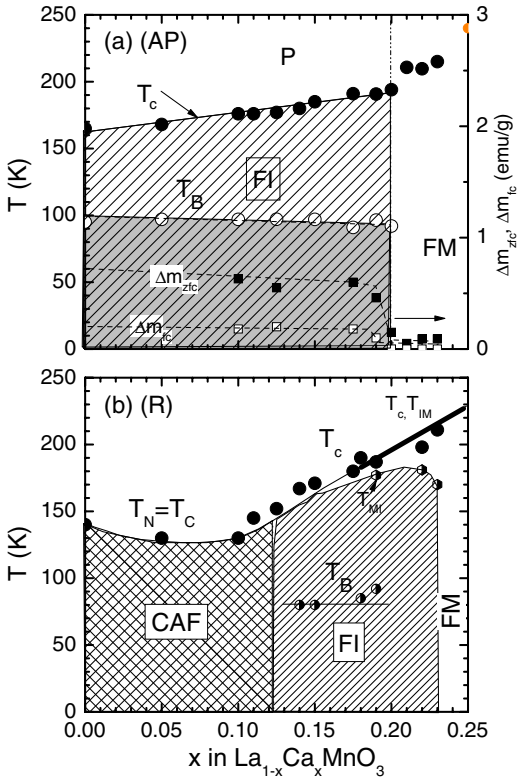

Figure 8. (a) The phase diagram for the air atmosphere (AP) prepared $La_{1-x}Ca_xMnO_3$ samples. The solid circles denote the paramagnetic–ferromagnetic transition. The open circles correspond to the onset temperature T_B of the jump in the ZFC dc magnetization curves. The open and closed squares show the temperature variation of the magnetization jump size during field cooling and zero-field cooling modes, respectively. (b) The phase diagram for R (He atmosphere annealed) $La_{1-x}Ca_xMnO_3$ samples. The solid circles denote the transition from the paramagnetic to the canted antiferromagnetic or ferromagnetic state. The half-filled circles for $x > 0.125$ correspond to the onset temperature T_B of the jump in the ZFC dc magnetization measurements. The half-filled hexagons show the metal–insulator transition temperature.

Having attributed the sharp peak below T_c in the middle of the insulating ferromagnetic regime to the Hopkinson effect (rapid increase of the magnetic anisotropy) we can conclude that the ferromagnetic insulating regime of the R samples is related to an increase in magnetic anisotropy. This increment reduces as the metallic boundary is approached. On the other hand, this anisotropy increases on approaching the canting antiferromagnetic boundary. This significant conclusion may be related to the idea of some kind of orbital ordering [29, 13] or orbital domains [30] occurring in the ferromagnetic–insulating regime. A new kind of orbital ordering below T_c for a sample with nominal composition $La_{0.85}Ca_{0.15}MnO_3$ has been proposed in [31]. At $T = 2$ K the high resolution neutron diffraction pattern is compatible with a monoclinic distortion described by the space group $P2_1/c$. In this structural model there are two non-equivalent MnO_2 layers alternating along the a-axis leading to a specific pattern of Mn–O distances, implying an unconventional type of orbital ordering. This model may be relevant to the ferromagnetic insulating state where a specific orbital ordering was proposed. However, the metallic resistivity variation of the particular sample questions the generalization of this model in describing the ferromagnetic insulating phase.

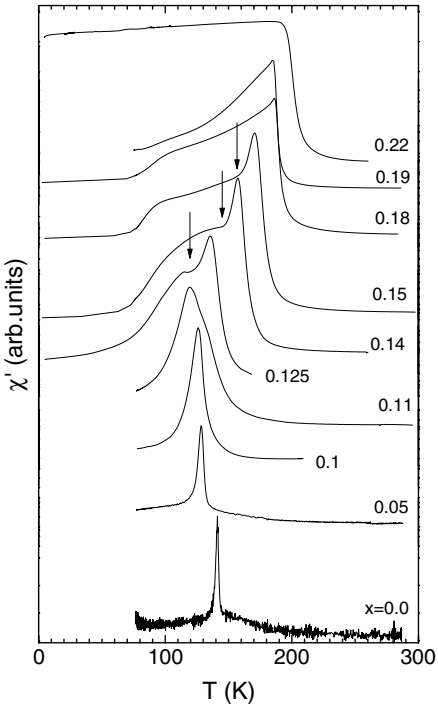

Figure 9. The temperature dependence of χ' for the R $La_{1-x}Ca_xMnO_3$ samples ($0 \leqslant x \leqslant 0.22$).

We must note that, as the magnetic measurements show, in the metallic regime ($x \geqslant 0.23$) no Hopkinson peak is present, which tells us that the magnetic anisotropy goes smoothly to zero at T_c. The AP samples do not show the Hopkinson peak at T_c, implying that the mechanism responsible for the anisotropy is not present in this case. Let us turn now to the feature at T_B. This feature is present for all the AP samples while it is less pronounced for the R samples. It is reasonable that for the R samples the anomaly at T_B in the magnetic measurements at low temperatures may be related to some kind of antiferromagnetic interaction as the CAF boundary is approached. These antiferromagnetic interactions may produce some glassiness with a diminishing contribution as the metallic boundary is approached. The detailed microscopic origin of the anomaly at T_B is not clear.

In some works the feature at T_B has been attributed to the sudden change of the domain wall dynamics due to domain wall pinning effects [32]. As has been observed, the small frequency dependence of the peak in χ'', at the temperature where the step occurs, is not an indication of spin glass behaviour. Many magnetically ordered systems exhibit frequency dependence without this implying spin glass behaviour. The dependence has been attributed to the freezing of domain wall motion which is a consequence of the rearrangements of electron states within the domain wall. The low field ZFC magnetization follows the changes in coercivity, which are directly related to the magnetocrystalline anisotropy. If this scenario is correct, then what is the origin of this sudden change in the magnetocrystalline anisotropy? Laiho *et al* [33], using air atmosphere prepared samples, using measurements of the frequency dependence of χ' in the region where the step was observed, attributed this feature to a re-entrant spin glass phase. It is well known that the compound with $x = 0.5$ undergoes a first-order charge/orbital ordering antiferromagnetic transition below the Curie temperature. This transition shows as a consequence a diminishing of the magnetization in both FC and ZFC magnetization branches,

something which is not observed in our measurements, where the ZFC and FC branches diverge for $T < T_B$.

The physics of the AP samples near $x = 0$ may be related to the results of Algarabel *et al* [34]. In this study, based on small angle neutron scattering data, it was suggested that the ferromagnetic phase (for $T < T_c$) is comprised of clusters increasing in size as the temperature decreases, reaching the value of 3–3.5 nm at low temperature. It is plausible that the non-stoichiometric samples, i.e. the AP ones, may consist of regions rich in holes (i.e. ferromagnetic) and poor in holes (with glass behaviour).

It is interesting to compare our results with those of Cheong and Chen [41]. Although in their review no details for the sample preparation are included, a direct comparison of the transition temperature curve reveals that our phase diagram for the R samples is in good agreement with those of [41]. The only difference is that the CAF–FI and FI–FM phase boundaries occur in slightly higher concentrations. The charge ordering phase in the ferromagnetic insulator regime proposed by the Cheong and Chen is still an open question which we cannot safely comment on.

The magnetic measurements of [36, 35] practically coincide with ours for the R sample with nominal composition $x = 0.15$. It is most probable that in their single crystal the stoichiometry is slightly lower than the nominal composition. For their particular crystal they observed a ferromagnetic–paramagnetic and a metal–insulator transition at $T_c \approx 180$ K, a ferromagnetic–insulator transition at $T_{FI} \approx 150$ K and a magnetic anomaly at $T_B \approx 95$ K, which is related to a levelling off of the resistivity.

Finally, it is interesting to compare the present magnetic measurements with those on $La_{1-x}Sr_xMnO_3$ in the ferromagnetic insulator regime occurring at $x = 0.125$. This compound exhibits a cooperative Jahn–Teller first-order transition at $T_{JT} \approx 270$ K, a second transition to a ferromagnetic metallic state at $T_c = 181$ K and then a final magnetostructural first-order transition to a ferromagnetic insulating state at $T_B = 159$ K. The transition at $T_B = 159$ K is characterized by a jump in the magnetization [19, 17, 37–39] typical for a first-order transition (delta function-like variation of the specific heat), the appearance of superstructure peaks, significant decrease of the orthorhombicity and convergence of the three characteristic Mn–O distances. In addition, Moussa *et al* [40] have found a splitting of the spin waves, an opening of a gap at $\mathbf{q} = (0, 0, 1/2)$ (*Pnmb* notation) and a locking of the spin wave energy on the energy values of phonons. All the above features, occurring at $T < T_B$, are indicative of a first-order transition, most probably related to a new orbital order [17].

Summarizing, in this work we have performed a systematic study of $La_{1-x}Ca_xMnO_3$ ($0 \leqslant x \leqslant 0.2$) aiming at advancing the knowledge of the underlying mechanisms which influence the structure and magnetic properties. The results of the present work clearly demonstrate that the physical properties of the low doped $La_{1-x}Ca_xMnO_3$ compounds depend on the oxygen partial pressure during preparation which influences the Mn^{4+} content. In order to prepare stoichiometric samples a low oxygen partial pressure is needed. The samples prepared in atmospheric conditions for $x < 0.16$ are cation deficient in such a way that the Mn^{4+} concentration remains constant regardless of x. The ferromagnetic insulating regime near the $x = 0.2$ boundary, for both families of samples, is not homogeneous.

References

[1] Wollan E O and Koehler W C 1955 *Phys. Rev.* **100** 545
[2] Goodenough J B 1955 *Phys. Rev.* **100** 564
[3] Schiffer P, Ramirez A P, Bao W and Cheong S W 1995 *Phys. Rev. Lett.* **75** 3336
[4] Ramirez A P, Schiffer P, Cheong S-W, Chen C H, Bao W, Palstra T T, Gammel P L, Bishop D J and Zegarski B 1996 *Phys. Rev. Lett.* **76** 3188

[5] Okuda T, Tomioka Y, Asamitsu A and Tokura Y 2000 *Phys. Rev.* B **61** 8009
[6] Biotteau G, Hennion M, Moussa F, Rodriguez-Carvajal J, Pinsard L, Revcolevschi A, Mukovskii Y M and Shulyatev D 2001 *Phys. Rev.* B **64** 104421
[7] Pissas M and Kallias G 2003 *Phys. Rev.* B **68** 134414
[8] Dagotto E, Hotta T and Moreo A 2001 *Phys. Rep.* **344** 1
[9] Kanamori J 1960 *J. Appl. Phys.* **31** 14S
[10] Kugel' K I and Khomskii D I 1982 *Sov. Phys.—Usp.* **25** 231
[11] Rodriguez-Carvajal J, Hennion M, Moussa F, Moudden A H, Pinsard L and Revcolevschi A 1998 *Phys. Rev.* B **57** R3189
[12] Moussa F, Hennion M, Biotteau G, Rodriguez-Carvajal J, Pinsard L and Revcolevschi A 1999 *Phys. Rev.* **60** 12299
[13] Van Aken B B, Jurchescu O D, Meetsma A, Tomioka Y, Tokura Y and Palstra T T M 2003 *Phys. Rev. Lett.* **90** 066403
[14] Lynn J W, Erwin R W, Borchers J A, Huang Q, Santoro A, Peng J L and Li Z Y 1996 *Phys. Rev. Lett.* **76** 4046
[15] Dai P, Fernandez-Baca J A, Wakabayashi N, Plummer E W, Tomioka Y and Tokura Y 2000 *Phys. Rev. Lett.* **85** 2553
[16] Fernandez-Baca J A, Dai P, Hwang H Y, Kloc C and Cheong S W 1998 *Phys. Rev. Lett.* **80** 4012
[17] Endoh Y, Hirota K, Ishihara S, Okamoto S, Murakami Y, Nishizawa A, Fukuda T, Kimura H, Nojiri H, Kaneko K and Maekawa S 1999 *Phys. Rev. Lett.* **82** 4328
[18] Yamada Y, Suzuki J, Oikawa K and Fernandez-Baca J A 2000 *Phys. Rev.* B **62** 11600
[19] Dabrowski B, Dybzinski R, Bukowski Z and Chmaissem O 1999 *J. Solid State. Chem.* **146** 448
[20] Huang Q, Santoro A, Lynn J W, Erwin R W, Borchers J A, Peng J L and Greene R L 1997 *Phys. Rev.* B **55** 14987
[21] Huang Q, Santoro A, Lynn J W, Erwin R W, Borchers J A, Peng J L, Ghosh K and Greene R L 1998 *Phys. Rev.* B **58** 2684
[22] Rodriquez-Carvajal J 1992 *Physica* B **192** 55
[23] Trukhanov S V, Kasper N V, Troyanchuk I O, Tovar M, Szymczak H and Bärnerer K 2002 *J. Solid State Chem.* **169** 85
[24] Moriya T 1963 *Magnetism I* vol 3, ed G T Rado and H Suhl (New York: Academic)
[25] Williams G 1991 *Magnetic Susceptibility of Superconductors and Other Spin Systems* ed R A Hein *et al* (New York: Plenum) p 475
Zhao J H *et al* 1999 *Phys. Rev.* B **59** 8391
[26] Chikazumi S 1964 *Physics of Magnetism* (New York: Wiley)
[27] Hong C S, Chi E O, Kim W S, Hur N H and Choi Y N 2003 *J. Phys. Soc. Japan* **71** 1583
[28] Mandal P and Ghosh B 2003 *Phys. Rev.* B **68** 014422
[29] Hennion M, Moussa F, Wang F, Rodríquez-Carvajal J, Mukovskii Y M and Shulyatev D 2001 *Preprint* cond-mat/0112159
[30] Papavassiliou G, Pissas M, Belesi M, Fardis M, Dolinsek J, Dimitropoulos C and Ansermet J P 2003 *Phys. Rev. Lett.* **91** 147205
[31] Lobanov M V, Balagurov A M, Pomjakushin V J, Fischer P, Gutmann M, Abakumov A M, Dỳachenko O G, Antipov E V, Lebedev O I and Van Tendeloo G 2000 *Phys. Rev.* B **61** 8941
[32] Joy P A and Date S K 2000 *J. Magn. Magn. Mater.* **220** 106
[33] Laiho R *et al* 2001 *Phys. Rev.* B **63** 094405
[34] Algarabel P A, De Teresa J M, Blasco J, Ibarra M R, Kapusta C, Sikora M, Zajac D, Riedi P C and Ritter C 2003 *Phys. Rev.* B **67** 134402
[35] Markovich V, Fita I, Puzniak R, Tsindlekht M I, Wisniewski A and Gorodetsky G 2002 *Phys. Rev.* B **66** 094409
[36] Markovich V, Rozenberg E, Shames A I, Gorodetsky G, Fita I, Suzuki K, Puzniak R, Shulyatev D A and Mukovskii Y M 2002 *Phys. Rev.* B **65** 144402
[37] Uhlenbruck S, Teipen R, Klingeler R, Büchner B, Friedt O, Hücker M, Kierspel H, Niemöller T, Pinsard L, Revcolevschi A and Gross R 1999 *Phys. Rev. Lett.* **82** 185
[38] Wagner P, Gordon I, Mangin S, Moshchalkov V V, Bruynseraede Y, Pinsard L and Revcolevschi A 2000 *Phys. Rev.* B **61** 529
[39] Liu G-L, Zhou J-S and Goodenough J B 2001 *Phys. Rev.* B **64** 144414
[40] Moussa F, Hennion M, Wang F, Kober P, Rodriguez-Carvajal J, Reutler P, Pinsard L and Revcolevschi A 2003 *Phys. Rev.* B **67** 214430
[41] Rao C N R and Raveau B (ed) 1998 *Colossal Magnetoresistance, Charge Ordering and Related Properties of Manganese Oxides* (Singapore: World Scientific) p 241